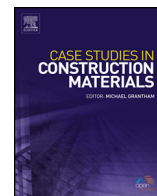




ELSEVIER

Contents lists available at ScienceDirect

Case Studies in Construction Materials

journal homepage: www.elsevier.com/locate/cscm

Case study

Use of burnt clay aggregate as phase change material carrier to improve thermal properties of concrete panel

Phattharachai Pongsopha^a, Piti Sukontasukkul^{a,*}, Tanakorn Phoo-ngernkham^b, Thanongsak Imjai^c, Pitthaya Jamsawang^d, Prinya Chindapasirt^e^a Construction and Building Materials Research Center, Department of Civil Engineering, King Mongkut's University of Technology North Bangkok, Thailand^b Department of Civil Engineering, Rajamangala University of Technology Isan, Nakhon Ratchasima, Thailand^c School of Engineering and Resources, Walailak University, Thailand^d Soil Engineering Research Center, Department of Civil Engineering, King Mongkut's University of Technology North Bangkok, Thailand^e Sustainable Infrastructure Research and Development Center, Department of Civil Engineering, Khon Kaen University, Thailand

ARTICLE INFO

Article history:

Received 17 January 2019

Received in revised form 9 April 2019

Accepted 11 April 2019

Keywords:

Phase change material

Burnt clay aggregates

PCM carrier

PCM impregnated aggregates

Thermal properties

ABSTRACT

In this research, the thermal properties of paraffin-impregnated burnt clay aggregate (PIA) concrete were studied. Paraffin was used as a phase change material (PCM) carrier and was incorporated into the burnt clay aggregates using heat and pressure. The compressive and flexural strengths of the concretes and the thermal insulation of the concrete panels were tested. The results of these tests revealed that the strengths and thermal insulation of the standard burnt clay aggregate concrete were improved with the use of PIA. The panels with PIA required more time to reach peak temperature and exhibited a larger drop in peak temperature relative to the control panel without PIA.

© 2019 The Authors. Published by Elsevier Ltd. This is an open access article under the CC BY license (<http://creativecommons.org/licenses/by/4.0/>).

1. Introduction

With growing concern over environmental problems, humans are focusing more on conserving natural resources and reducing negative environmental impacts. There is a need to focus on the issue of energy conservation. In 2009, a UN publication (Sustainable Buildings and Climate Initiative) reported that the building sector (both residential and commercial) was responsible for approximately 40% of primary global energy consumption [1]. In resident buildings, most of the energy was used for heating and air conditioning. On a daily basis, people spend a significant amount of time inside buildings or structures, and if the thermal properties of construction materials can be enhanced, the consumption of energy for heating and air conditioning can be reduced.

Concrete is the most widely used construction material due to its availability and low cost. There are several strategies for enhancing the thermal performance of concrete buildings. A conventional approach involves adjusting the mass of the building envelope, since the thermal storage potential of a building increases with increased building mass. This mass increase prolongs the duration of heat transfer and increases the time required to reach peak temperature. However, modern design trends are moving toward thinner and lighter-weight structures, and increasing the envelope thickness has several

* Corresponding author.

E-mail addresses: s6001081913010@email.kmutnb.ac.th (P. Pongsopha), piti.s@eng.kmutnb.ac.th, piti@kmutnb.ac.th (P. Sukontasukkul), tanakorn.ph@rmuti.ac.th (T. Phoo-ngernkham), thanongsak.im@wu.ac.th (T. Imjai), pitthaya.j@eng.kmutnb.ac.th (P. Jamsawang), prinya@kku.ac.th (P. Chindapasirt).

disadvantages that are often considered unsuitable. Therefore, in order to enhance the thermal performance of concrete buildings with minimal changes in the existing building envelope, the use of a novel concrete containing passive or active thermal enhancing components (such as air bubbles, phase change material, or integrated hydronic systems) would be beneficial. The major benefit of using a phase change material (PCM) is that it allows structures to improve their thermal storage capabilities through improvements in their latent heat captivity with minimal change to the existing building design [2]. Several studies have shown that the ability of PCMs to absorb and release heat during the phase change process can be utilized by storing the heat inside the structures and slowing down the rate of heat transmission (shifting the temperature peak period) [3–7].

Briefly, the use of PCMs in house envelopes began around 1947, when PCM (Glauber's salts in steel drums) was first incorporated into the building components of a house in Dover, Massachusetts [8]. In cool weather, the PCM absorbed heat from the surrounding environment during the day and then released the stored energy during the night to prevent the building from becoming excessively cold [9,10]. In hot weather, the ability of the PCM to absorb heat helped reduce heat flow through the building and shifted the peak cooling loads to the off-peak period, thereby balancing and reducing energy consumption [11–13]. There are three groups of PCMs: organic, inorganic and eutectic [7]. The organic group consists of materials such as paraffin and some fatty acids. These materials exhibit the following properties: congruent melting (melting and freezing repeatedly without phase segregation and consequent degradation of their latent heats of fusion), and self-nucleation (crystallizing with little or no supercooling and usually noncorrosive).

Applications of these PCMs in concrete materials began around 1980 with concrete masonry blocks. Several researchers proposed using masonry blocks as PCM carriers by incorporating the PCM into concrete masonry blocks using various methods [17–19]. Some examples of these methods include incorporating the PCM by immersion, hollow core containment [20], dry mixing, and imbibing the PCM into porous materials [21]. However, there were also concerns over issues such as volume changes, slow rate of heat transfers on organic PCM products, leakage, and negative side effects on the properties of the masonry blocks.

In the case of cast-in-place concrete materials, there are several methods to incorporate the PCM into a concrete mixture. One approach is to directly mix the PCM with the concrete mixture as one of the constituent materials or as a replacement for one of the constituent materials (i.e., sand). However, this method was found to have drawbacks related to changes in the material matrix, interactions with the cement paste and possible leakage over its lifetime [22]. To solve the leakage problem, the encapsulation technique was introduced [23]. Using this technique, the PCM is encapsulated inside small spherical capsules and then mixed with concrete [24–28]. However, there are some drawbacks related to interactions with the cement matrix, cost effectiveness, and the manufacturing process.

In this study, burnt clay coarse aggregate (BCA) was used as a PCM carrier. The liquid PCM, paraffin, was incorporated into the aggregate using heat and pressure. Concrete panels with paraffin-impregnated burnt clay aggregates (PIA) were tested in actual field conditions for 72 h using a cubicle box. The results in terms of temperature and time differences were recorded and discussed.

2. Experimental procedure

2.1. Materials

The materials used in this study consisted of Portland Cement Type I, river sand, and burnt clay aggregate (BCA). The properties and particle shape of the BCA are shown in Table 1. The properties of paraffin, which was used as a PCM, are shown in Table 2.

Table 1
Properties and particle shape of burnt clay aggregate.


Properties (unit)		Particle Shape
Unit weight (kg/m^3)	732	
Percent of voids (%)	72	
Bulk specific gravity (Dry)	1.08	
Bulk specific gravity (SSD)	1.25	
Apparent specific gravity	1.30	
Percent Absorption (%)	16.0	

Table 2
Properties of Paraffin.

Properties (unit)	Standard	Value
Melting Point (°C)	ASTM D87-09	57.2–59.9
Oil Content (%)	ASTM D721-15	0.4
Penetration at 25 °C	ASTM D1321-16a	10.0–17.0
Color	ASTM D156-15	30
UV Absorption	FBA 178.3710	1.3

2.2. Experimental procedure

2.2.1. PCM impregnation

The conditions for the impregnation of BCA with paraffin using heat and pressure were optimized. In the first step, the impregnation was done with heat only, at 80, 100 and 120 °C. The aggregates were oven-dried and maintained at the desired temperature prior to the impregnation. The paraffin was melted in a pan and then placed in the oven. The aggregates were submerged in the liquid paraffin at a constant temperature. The heat and pressure processes were carried out at temperatures of 100 and 120 °C and pressures of 34.5, 69.0 and 103.5 kPa. The aggregates were conditioned and submerged in the liquid paraffin at constant temperature and pressure. The aggregate samples were removed from the chamber every hour to measure their weights. The changes in weight were calculated to determine the levels of impregnation. After the impregnation, the specific gravity and absorption of the aggregates were tested in accordance with ASTM C127-15.

2.2.2. Casting and testing of PIA concretes and panels

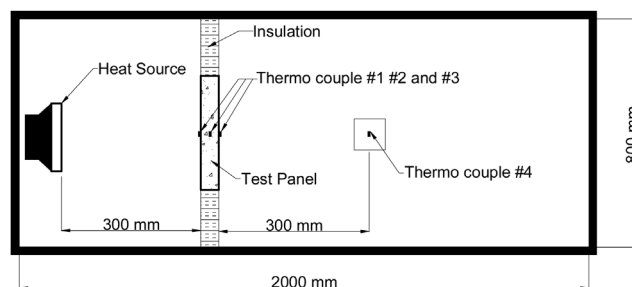
Using the results from 2.2.1, the paraffin-impregnated burnt clay aggregate (PIA) with the highest level of impregnation was selected to use as a coarse aggregate for making the concrete panels. The mix proportions of the concretes are shown in Table 3. After mixing, the concrete densities were determined in accordance with ASTM C138/C138M-17. The fresh concretes were then cast into 150 × 150 × 150 mm cube molds and 100 × 100 × 350 mm prism molds in accordance with BS EN 12390-1:2012 and ASTM C78/C78M-16, respectively. The specimens were demolded at the age of 1 day and kept in water until the testing age. The fresh concretes were also cast into 400 × 400 × 50 mm and 400 × 400 × 100 mm molds for the heat insulation tests. Three thermocouples were installed in each specimen during casting. The specimens were demolded at the age of 1 day and wrapped with plastic sheeting until the testing age.

The compressive strengths of the concrete specimens were tested at the age of 28 days using 150 × 150 × 150 mm cubes in accordance with BS EN 12390-1:2012. In addition, at the age of 28 days, the 100 × 100 × 350 mm prisms were tested in flexure using third-point loading in accordance with ASTM C78/C78M-16, and the modulus of rupture values were determined. The reported results are the averages of three samples.

To evaluate the temperature performance of the specimens, heat insulation tests were carried out in the laboratory and in the field. In the laboratory, the tests were carried out using the heat insulating chamber constructed at KMUTNB (Fig. 1). The chamber, which has dimensions of 800 × 800 × 2000 mm, is constructed of steel plates and is covered inside with insulating sheets. The chamber is equipped with a heat source (1500 W spotlight), specimen supporter and

Table 3
Concrete mix proportions.

Concrete ID	Cement (kg)	Sand (kg)	Water (kg)	BCA (kg)	PIA (kg)
BCA	477	669	200	488	0
PIA	477	669	200	0	488

**Fig. 1.** Setup for heat insulation test in laboratory.

thermocouples, as shown in Fig. 1. The specimens were prepared from square panels and had dimensions of $400 \times 400 \times 50$ mm. Three thermocouples were embedded in the specimen at different locations to measure the temperature changes at the front, mid-panel and inner surfaces. One thermocouple was installed inside the chamber (300 mm from the specimen) to measure the room temperature changes. The temperature change was measured and recorded automatically every 5 s using a standalone data logger. The temperature pattern was established as a one-cycle test in which heat was supplied to the plate until the temperature at the mid plate reached 60 ± 3 °C, and then the heating ceased. Temperature measurement continued for approximately 5000 s after the peak temperature was reached.

The field tests were carried out using a cubicle constructed of aerated concrete with an inside air volume of $200 \times 200 \times 500$ mm³, as shown in Fig. 2. The cubicle was placed in a location without shade to avoid any sun-blocking during the experiment. The test specimen was placed on top of the cubicle. To prevent contact between the test specimen and the supporting box and avoid heat transfer, a strip of insulating sheet was placed between the contact surfaces of the test panel and the supporting cubicle. Four thermocouples were used to monitor the changes in temperature of the panel and inside the cubicle, as shown in Fig. 2. The temperatures were measured and recorded automatically every 5 s using a stand-alone automatic data acquisition system. Each test was carried out in outdoor conditions for 72 h (3 day/night cycles).

3. Results and discussion

3.1. Impregnation percentage and aggregate properties

A typical curve of the relationship between impregnation level and time of impregnation is shown in Fig. 3. The initial impregnation percentage due to self-sorptivity observed immediately after the submerging of the aggregate into the liquid paraffin was approximately 7%. The impregnation percentage then increased gradually (increasing stage) and reached a constant level (steady stage).

The results of impregnation under heat only are shown in Fig. 4. As expected, the impregnation increased with the increase in temperature. The impregnation levels at temperatures of 80, 100 and 120 °C were 14.0, 14.5 and 15.0%, with corresponding impregnation times of 10, 9 and 7 h. With combined heat and pressure, the aggregates were able to absorb more paraffin in a shorter period of time. The highest impregnation percentage of 16.1% by weight, with an impregnation time of 2 h, was obtained at a temperature of 120 °C and a pressure of 103.5 KPa, as shown in Fig. 5.

Fig. 6 shows the comparison between the specific gravity and absorption of the PIA with 16.1% impregnation (120 °C and 103.5 KPa) and those of standard BCA. The PIA exhibited higher dry specific gravity, saturated surface dry specific gravity and apparent specific gravity values than those of BCA due to the impregnation by paraffin. For example, the specific gravity of saturated surface dry PIA was 1.303, compared to 1.234 for BCA. The impregnation reduced the aggregate absorption from 16.2% to 0.2% by filling the pores in the aggregates.

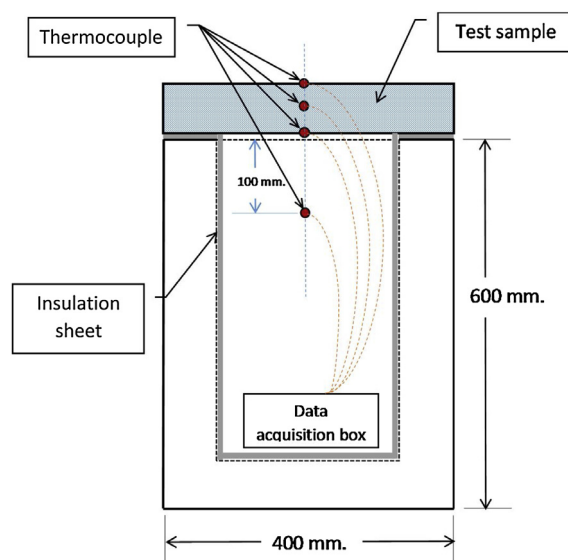


Fig. 2. Cubicle for heat insulation in field test.

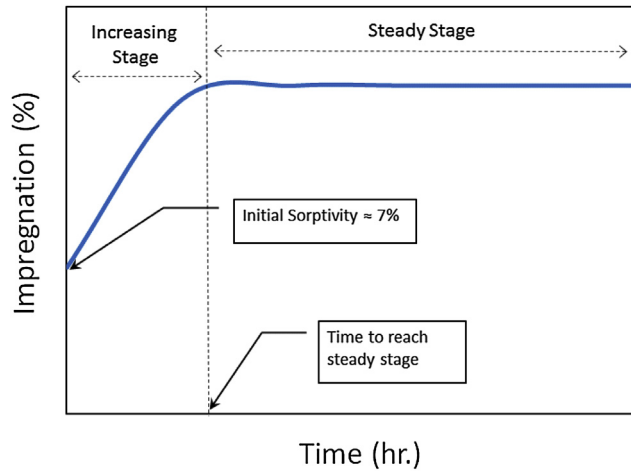


Fig. 3. Typical impregnation and time relationship.

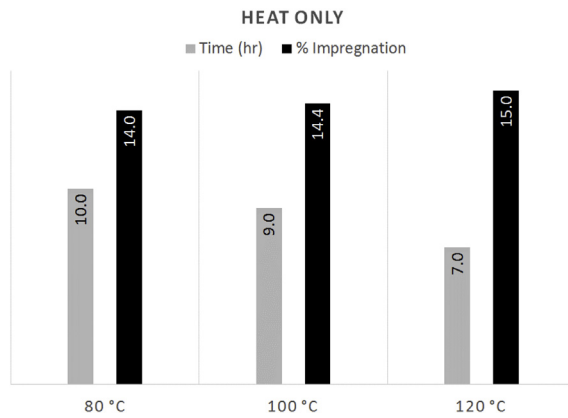


Fig. 4. Impregnation percentage and time for heat only.

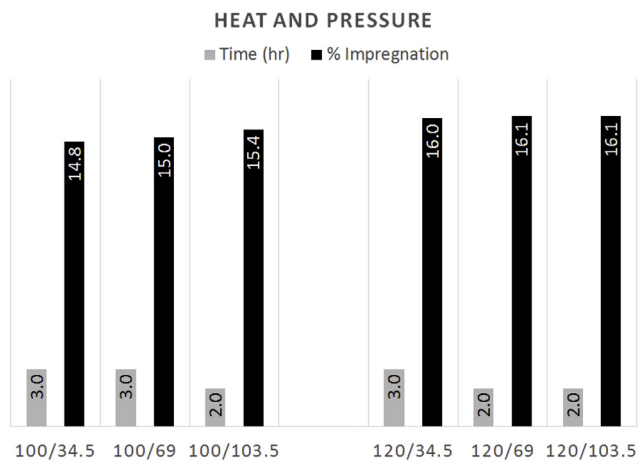


Fig. 5. Impregnation and time for heat and pressure processes.

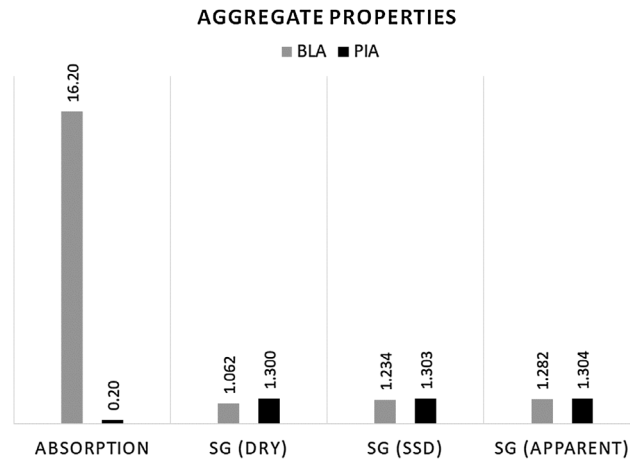


Fig. 6. Properties of BCA and PIA Aggregates.

3.2. Concrete properties

3.2.1. Density, absorption and compressive strength

The aggregates with the highest impregnation percentage of 16.1% (120 °C and 103.5 KPa) were used in making the concrete. The results of the tests of BCA and PIA concretes are shown in Fig. 7. With the use of PIA, the compressive strength increased significantly from 23.6 to 29.9 MPa, and the modulus of rupture also increased from 3.88 to 4.20 MPa. This was due to the increased density of the aggregates as the paraffin filled the aggregate voids. In addition, with denser aggregates, the density of the concrete increased from 1563 to 1785 kg/m³ and the absorption decreased from 1.45 to 0.96%. Memon et al. [29] reported a similar increase in the compressive strength from 7 to 14% in concrete containing PCM aggregates from 50 to 100% by volume compared to those containing normal aggregates.

3.2.2. Heat insulation properties

3.2.2.1. Laboratory test. Results from the laboratory tests are shown in Fig. 8a–c. Considering the temperature changes at the mid-plate location, where the maximum temperature was controlled at 60 °C, the difference in time required to reach peak temperature can be seen from the test result. The time required for the BCA panel to reach peak temperature was 2368 s (Table 4), and for the panel with paraffin aggregates (PIA), the time was extended by approximately 900 s–3252 s. The time increase demonstrates the ability of the PCM to absorb heat during the phase change process.

The temperature patterns of the inner surface and inside the chamber were different than that of the outer surface. In addition to the increase in time to reach peak temperature, a decrease in peak temperature was observed. The peak temperatures of the PIA at the inner surface and inside the chamber were found to be lower than those of BCA by approximately 2 and 0.7 °C, respectively (Table 4).

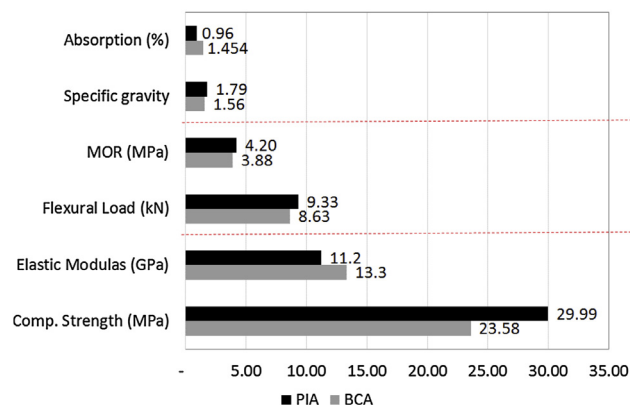
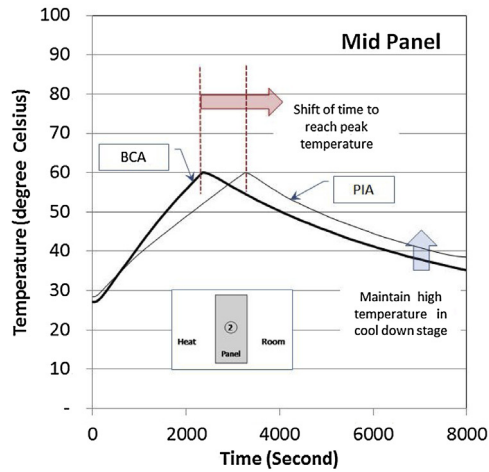
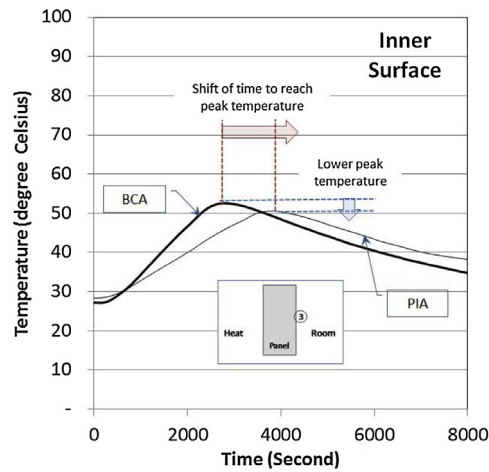


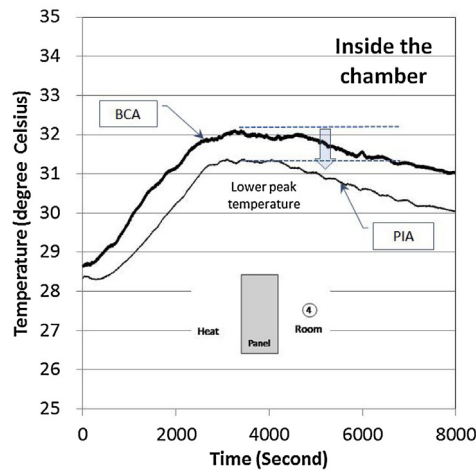
Fig. 7. Properties of PIA and BCA concretes.



(a)



(b)



(c)

Fig. 8. Temperature Change vs. Time (Laboratory).

Table 4
Peak temperature and Time to reach Peak temperature (Laboratory).

Type	Category	Location		
		Mid	Inner	Inside
BCA	Temp (°C)	60.0	52.6	32.1
	Time (s)	2368	2772	3391
	Rate (°C/min)	1.52	1.14	0.57
PIA	Temp (°C)	60.0	50.6	31.4
	Time (s)	3252	3,813	3,683
	Rate (°C/min)	1.11	0.80	0.51

Using the peak temperature and time, the rate of heat transfer can be calculated, as shown in Table 4. The results show that the rate of heat transfer of the PIA was slower than that of the BCA at every location. The slower rate of heat transfer is the direct result of PCM absorbing heat without increasing the surrounding temperature. Similar findings were reported by Rao et al. [30] and Üрге-Vorsatz et al. [31].

3.2.2.2. Field test. The field tests were carried out during the months of April and May with outdoor temperatures between 28 and 40 °C. The measured temperatures of the tested cubicle were between 28 and 56 °C. The typical temperature patterns measured for the four locations are shown in Fig. 9. Similar to the outdoor temperature patterns, the temperatures began rising at approximately 8:00 am. However, the time to reach peak temperature at each location was different, depending on the distance from the top surface. At the top (outer) surface of the panel (1), the peak temperature was reached at approximately the same time as that of outdoor temperature, approximately 13:20–14:00 pm. At the mid-surface (2), the bottom (inner) surface (3) and the inside the chamber (4) locations, there were delays of peak temperatures as well differences in peak temperatures. Immediately following its peak, the temperature began to decrease, and most of the heat was lost at approximately midnight. Afterward, there was a slow cooling period, and the lowest temperature was reached at approximately 6:00 AM.

The testing was carried out for two months during the summer. However, there were variations in temperature from day to day and from test to test. To compare the results, it was necessary to convert the obtained data to sets of comparable data. In this case, the relative temperature ratio (ratio between the temperature at any time and maximum temperature) was introduced and is shown in Fig. 10. This approach allowed a direct comparison of the temperature variations from day to day and test to test.

3.2.2.3. Comparison between BCA and PIA panels. Fig. 11 shows a comparison of the typical relative temperature patterns of the BCA and PIA panels. At the outer surface, the incorporation of PCM caused a difference in the time to reach peak

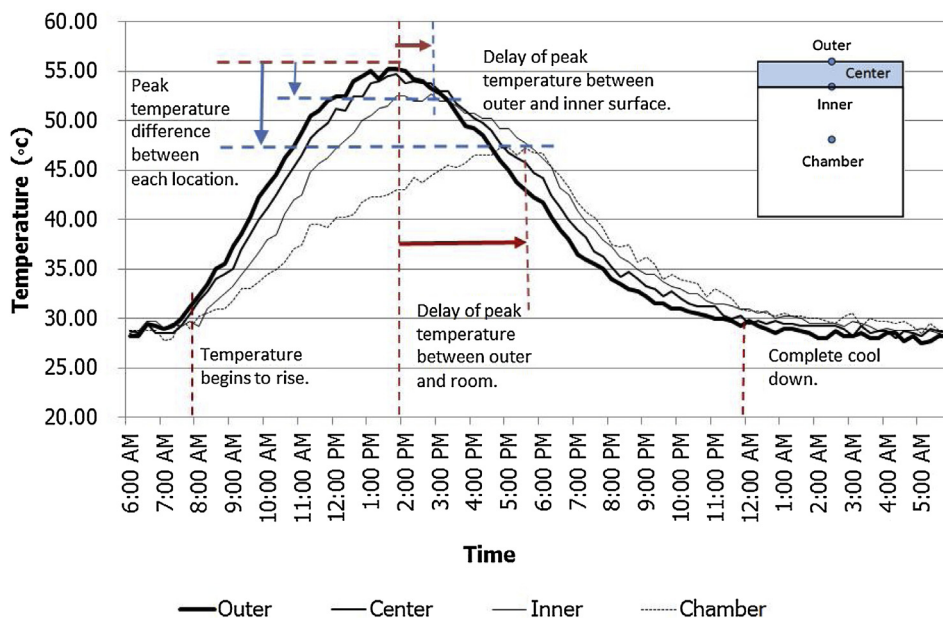


Fig. 9. Typical measured temperatures of the panel and inside the chamber.

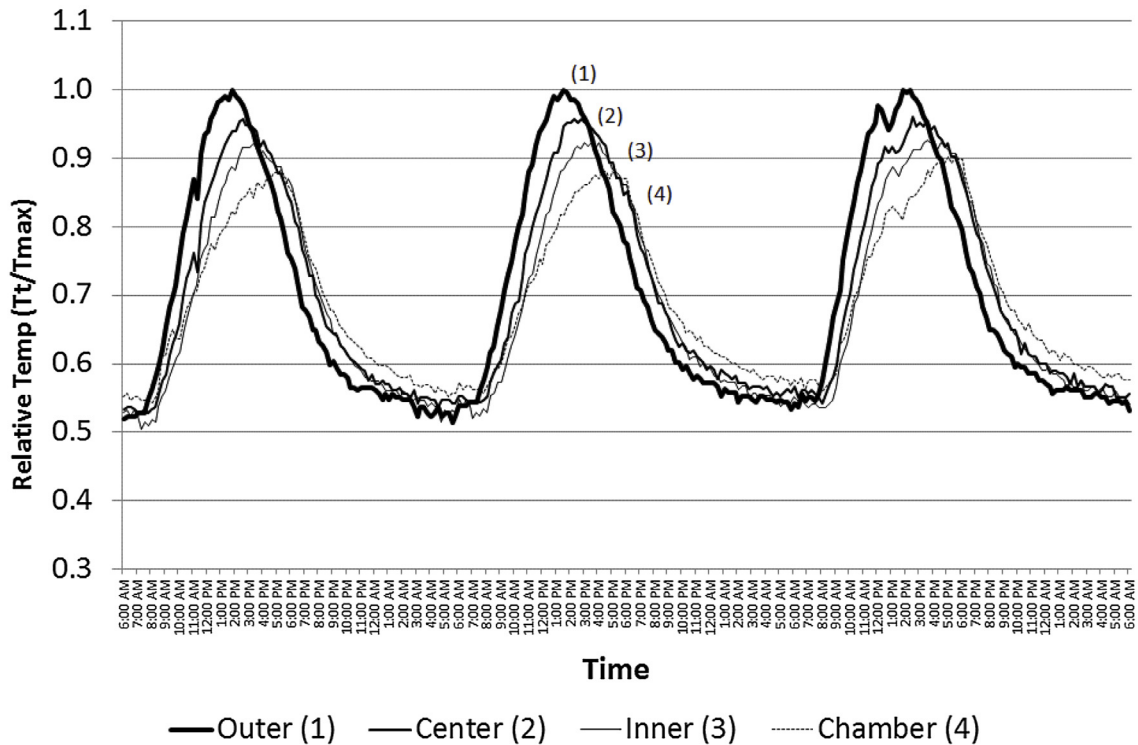


Fig. 10. Typical relative temperature of PIA panel and inside the chamber.

temperature (TD). Inside the chamber, the effect of PCM created both a TD and a difference in peak temperature (DP). Both effects primarily resulted from the thermal insulation properties of the concrete. In the PIA panels, the temperature increase was delayed, and the chamber temperature reached its peak temperature after the outdoor peak temperature had passed. This effect thus lowered the peak temperature inside the chamber.

To compare the panel performances, the temperatures at three different locations, viz., outer surface of the panel (1), inner surface of the panel (3), and inside the chamber (4), were used. The average time at peak temperature, time differences to reach peak temperature (TD) and the differences in peak temperature (DP) were obtained, as shown in Table 5. The time to reach peak temperature depended on the location and the panel thickness. For the 50 mm thick BCA panels, the average TD between the outer and inner surfaces of the panel (TD3) was 10 min, and the average TD between the outer surface of the panel and inside the chamber (TD4) was 1:50 h. For the 100 mm thick BCA panels, the differences were increased to 1:45 and 3:00 h, demonstrating the effect of the increase in thermal mass on the duration of heat transfer. The increase in thermal mass (thickness) resulted in the increase in the duration of heat transfer.

Regarding the performances of the BCA and PIA panels, the PIA panels exhibited longer TDs and larger DPs than those of the BCA panels. For example, the average TD values for the PIA/100 mm panels were 2:10 and 4:00 h compared to 1:45 and 3:00 h for the BCA/100 mm panels. The longer TDs indicated that the PIA was able to slow the rate of heat transfer as a result of the ability of phase change to reduce the heat inside the chamber.

The panel thickness played an important role in the DP values. For the 50 mm thick panels, the difference in the DP values was small, with DP values of 5.08 and 5.25 °C for the BCA and PIA panels, respectively. However, for the 100 mm thick panels, the effect of PCM was significant. The average DP values of the BCA and PIA panels were 5.67 and 7.00 °C, respectively, resulting in a difference of 1.33 °C. The increased temperature difference demonstrated the effectiveness of PIA for lowering the temperature inside the chamber. These results agree with the results obtained by Sukontasukkul [32] when PCM was mixed with plastering mortar and placed on a brick wall cubical. Their tests were carried out for 5 days/nights, and the temperature inside the cubicle with PCM (polyethylene glycol type) was found to be lower than that of the other cubicles.

4. Conclusion

The experimental results showed that the burnt clay aggregate (BCA) is suitable for use as an effective PCM carrier. The incorporation of paraffin into the BCA with heat and pressure was effective. The high paraffin impregnation percentage of 16.1% was obtained using heat at 120 °C and a pressure of 103.5 KPa, which resulted in enhanced basic properties, viz., increased specific gravity and reduced absorption. The obtained paraffin-impregnated burnt clay aggregate (PIA) was able to

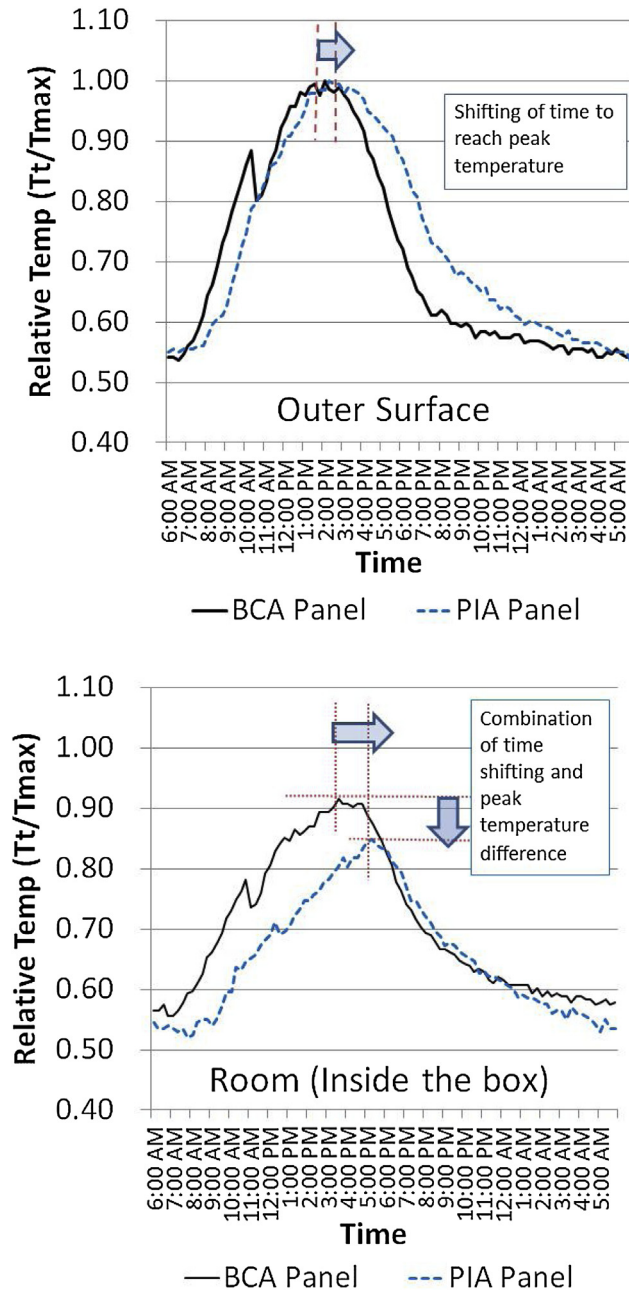


Fig. 11. Typical relative temperature of BCA and PIA panels.

Table 5

Average time at peak temperature, time difference to reach peak temperature and difference in peak temperature.

Aggregate type/Panel thickness	Average time at peak temperature (h: min)			Time difference to reach peak temp. (TD) (h:min)		Difference in peak temp. (DP) (°C)	
	Top of panel (1)	Bottom of panel (3)	Inside chamber (4)	TD3 (3)-(1)	TD4 (4)-(1)	DP3 (3)-(1)	DP4 (4)-(1)
BCA/50 mm	14:00	14:10	15:50	0:10	1:50	1.42	5.08
BCA/100 mm	13:40	15:25	17:05	1:45	3:00	3.50	5.67
PIA/50 mm	13:22	14:22	15:52	1:00	2:30	2.00	5.25
PIA/100 mm	13:20	15:30	16:50	2:10	4:00	2.75	7.00

enhance the thermal insulation properties of concrete panels and provided the additional benefit of increased compressive and flexural strengths of the concretes. For the thermal insulation properties, the benefit of using PIA was twofold. First, the time difference to reach peak temperature was increased. This increase resulted in the concrete buildings with PIA having longer periods of lower temperature, since the peak temperatures were delayed. Second, the difference in peak temperatures between the outside and the inside of concrete buildings was increased, resulting in lower temperatures inside the concrete buildings. The results also indicated that the thick PIA panel (100 mm) performed significantly better than the thin panel (50 mm).

Conflict of interest

Author declares that they have no conflict of interest.

Acknowledgements

This work is financially supported by 1) King Mongkut's University of Technology North Bangkok, Contract No. 61-PHD-013 and 2) Thailand Research Fund (TRF) under the TRF Distinguished Research Professor Grant No. DPG618002. The authors also would like to thank Siamese Ecolite Co., Ltd. for the supply of lightweight aggregates and all senior students involved in the project.

References

- [1] Buildings and Climate Change: A Summary for Decision Makers, United Nations Environmental Programme, Sustainable Buildings and Climate Initiative, Paris, 2009.
- [2] S.K. Sharma, Zero energy building envelope components: a review, *Int. J. Eng. Res. Appl.* 3 (2) (2013) 662–675 ISSN: 2248-9622.
- [3] A. Abhat, Low temperature latent heat thermal energy storage, heat storage materials, *Sol. Energy* 30 (1983) 313–332.
- [4] H.G. Lorsch, K.W. Kauffman, J.C. Denton, Thermal energy storage for heating and air conditioning, future energy production system, *Heat Mass Transfer Proc.* 1 (1976) 69–85.
- [5] A. Abhat, et al., Development of a Modular Heat Exchanger With an Integrated Latent Heat Storage, Report No. BMFT FBT 81-050, Germany Ministry of Science and Technology Bonn, 1981.
- [6] D.V. Hale, M.J. Hoover, M.J. O'Neill, *Phase Change Materials Handbook*, Marshal Space Flight Center, Alabaa, 1971.
- [7] A. Sharma, V. Tyagi, C.R. Chen, D. Buddhi, Review on thermal energy storage with phase change materials and applications, *Renew. Sustain. Energy Rev.* 12 (2009) 318–345.
- [8] M. Telkes, Solar house heating—a problem of heat storage, *J. Heat Ventilating* 44 (1947) 68–75.
- [9] M. Telkes, Trombe wall with phase change storage material, *Proceedings of the 2nd National Passive Solar Conference* (1978).
- [10] G.A. Frysinger, J. Sliwkowski, Phase Change Material Storage Assisted Heating Systems, University of Delaware, USA. PH-87-5, No. 4, 1987 p. 516.
- [11] S.D. Sharma, K. Sagara, Latent heat storage materials and systems: a review, *Int. J. Green Energy* 2 (2005) 1–56 ISSN: 0197-1522.
- [12] J. Kośny, E. Kossecka, Understanding a potential for application of phase-change materials (PCMs) in building envelopes, *ASHRAE Trans.* 119 (2013) 1 (Part 1. DA-13-001).
- [13] K. Childs, T. Stovall, Potential Energy Savings Due to Phase Change Material in a Building Wall Assembly: An Examination of Two Climates. Report—ORNL/TM-2012/6 March 2012, Oak Ridge National Laboratory, USA, 2012.
- [14] J.D. Balcomb, C.E. Kosiewicz, G.S. Lazarus, R.D. McFarland, W.O. Wray, *Passive Solar Design Handbook*, vol. 3, Los Alamos National Lab., 1983 ISBN 0-89553-106-2.
- [15] I.O. Salyer, A.K. Sircar, Phase change materials for heating and cooling of residential buildings and other applications, *Proceedings of the 25th Intersociety Society Energy Conversion Engineering*, (1990) , pp. 236–243.
- [16] D.W. Hawes, D. Feldman, Latent heat storage in building materials, *Energy Build.* 20 (1993) 77–86.
- [17] I.O. Salyer, A.K. Sircar, Advanced phase change materials technology: evaluation in lightweight solite hollow-core building blocks, *Proceedings of the 30th Intersociety Energy Conversion Engineering Conference* (1995) 217–224.
- [18] I.O. Salyer, A.K. Sircar, Development of PCM Wallboard for Heating and Cooling of Residential Buildings, *Thermal Energy Storage Research Activities Review*, U.S. Department of Energy, New Orleans, 1989, pp. 97–123.
- [19] P. Schossig, H. Henning, S. Gschwander, T. Haussmann, Microencapsulated phase change materials integrated into construction materials, *Sol. Energy Mater. Sol. Cells* 89 (2005) 297–306.
- [20] M.N.A. Hawlader, M.S. Uddin, M.M. Khin, Microencapsulated PCM thermal-energy storage system, *Appl. Energy* 74 (2003) 195–202.
- [21] A. George, Hand book of thermal design, in: C. Guyer (Ed.), *Phase Change Thermal Storage Materials*, McGraw Hill Book Co., 1989 [chapter 1].
- [22] V.V. Tyagi, S.C. Kaushik, S.K. Tyagi, T. Akiyama, Development of phase change materials based microencapsulated technology for buildings: a review, *Renew. Sustain. Energy Rev.* 15 (2011) 1373–1391.
- [23] L.F. Cabeza, C. Castellon, M. Nogues, M. Medrano, R. Leppers, O. Zubillaga, Use of microencapsulated PCM in concrete walls for energy savings, *Energy Build.* 39 (2007) 113–119.
- [24] B. Boh, B. Sumiga, Microencapsulation technology and its applications in building construction materials, *RMZ—Mater. Geovviron.* 55 (3)(2008) 329–344.
- [25] M.N.A. Hawlader, M.S. Uddin, M.M. Khin, Microencapsulated PCM thermal energy storage system, *Appl. Energy* 74 (2003) 195–202.
- [26] Shazim Ali Memon, H.Z. Cui, Hang Zhang, Feng Xing, Utilization of macro encapsulated phase change materials for the development of thermal energy storage and structural lightweight aggregate concrete, *Appl. Energy* 139 (2015) 43–55.
- [27] V.V. Rao, R. Parameshwaran, V.V. Ram, PCM-mortar based construction materials for energy efficient buildings: a review on research trends, *Energy Build.* 158 (2018) 95–122.
- [28] Diana Ürge-Vorsatz, Luisa F. Cabeza, Susana Serrano, Camila Barreneche, Ksenia Petrichenko, Heating and cooling energy trends and drivers in buildings, *Renew. Sustain. Energy Rev.* 41 (2015) 85–98.
- [29] P. Sukontasukkul, T. Sutthiphasilp, W. Chalodhorn, P. Chindaprasirt, Improving thermal properties of exterior plastering mortars with phase change materials with different melting temperatures: paraffin and polyethylene glycol, *Advances in Building Energy Research*, (2018), pp. 1–21, doi:http://dx.doi.org/10.1080/17512549.2018.1488614.